Journal of Rock Mechanics and Geotechnical Engineering 13 (2021) 154–166

Contents lists available at ScienceDirect

Journal of Rock Mechanics and Geotechnical Engineering

journal homepage: www.jrmge.cn

Full Length Article

An integrated laboratory experiment of realistic diagenesis, perforation and sand production using a large artificial sandstone specimen

Ashirgul Kozhagulova [a,*], Ainash Shabdirova [a], Nguyen Hop Minh [b], Yong Zhao [a]

[a] School of Engineering and Digital Sciences, Nazarbayev University, 53 Kabanbay Batyr Avenue, Nur-Sultan, Kazakhstan
[b] Fulbright University Vietnam, 105 Ton Dat Tien, Ho Chi Minh City, Viet Nam

ARTICLE INFO

Article history:
Received 22 January 2020
Received in revised form
12 August 2020
Accepted 9 September 2020
Available online 6 November 2020

Keywords:
Sand production
Equipment development
Geotechnical testing
Weak sandstone formations
New testing procedure

ABSTRACT

Sand production is, a challenging issue in petroleum industry, mainly associated with weak unconsolidated formations. A novel testing procedure and a new apparatus were developed to conduct an integrated experiment of diagenesis, perforation and sand production on a single large cylindrical artificial sandstone specimen, where solid and fluid pressures can be independently controlled such that realistic reservoir historical conditions can be well simulated in the laboratory. Fluid injection can be performed in both radial and vertical directions, where both single- and two-phase flows can be implemented for study of sand production behaviors at different reservoir's maturity stages. The equipment consists of an intensive instrumentation system to monitor pressures, displacements and material states continuously. The produced sand particles were filtered and monitored in real-time for the study of time-dependent phenomena. The experimental results showed similar patterns to that observed in the field and provided valuable insight for the development of prediction methods for sand production of similar materials.

1. Introduction

In many countries across the world, oil and gas energy consumption pays a critical role in their economy. One of the challenging issues in oil and gas extraction is the sanding scenario associated with ultra-weak and weak formations with compressive strength values up to 3.5 MPa and 28 MPa, respectively (Wu et al., 2016). Sand production is an undesirable process of producing sand along with crude oil. When a well is drilled, cased and perforated, a damaged zone is developed near the well wall due to stress redistribution. When the oil flow is produced through this damaged zone, particles can detach from the rock matrix and migrate towards the wellbore, which leads to changes in the rock properties near the wellbore region. The produced sands contribute significantly to the erosion of downhole and surface equipment during their interaction with the metal surface of structures, causing additional operational costs. In the severe cases of massive sand production, the wellbore may collapse, leading to well abandonment. Restoring the damaged zone and lowering oil production to minimize sand production both cause an adverse impact on the economic aspect of the operation. In order to minimize solid production from the weak or ultra-weak formation, a strategy of oil field development is required for proper sand management based on reliable prediction methods of sand production.

In order to understand sand production pattern under different conditions, laboratory experiments were conducted to investigate controlling parameters in terms of fluid flow rate, pressure drawdown, material properties and solid stress. The first scientific experiments related to sand production started in the 1930s by Terzaghi (1936), who first observed sand arch around a bottom trapdoor in the box filled with sand. His experiment was improved by Hall and Harrisberger (1970), who discovered a correlation between the formation of sand arches and the introduced fluid flow. Later experiments (Tronvoll et al., 1993, 1997; Nicholson et al., 1998; Papamichos et al., 2000; Fattahpour et al., 2012; Wu et al., 2016) were conducted under different oil production parameters, and sand production was found to be dependent of formation rock material, saturation and injection fluid, stress anisotropy and stress level.

The quality of the experimental work is dependent on the reconstitution of real conditions in a controlled manner. Due to

* Corresponding author.
E-mail address: ashirgul.kozhagulova@nu.edu.kz (A. Kozhagulova).
Peer review under responsibility of Institute of Rock and Soil Mechanics, Chinese Academy of Sciences.

https://doi.org/10.1016/j.jrmge.2020.09.004

difficulty associated with retrieving rock cores, sand production tests were usually conducted on artificial cores, which showed good convergence with real cores in terms of mechanical behavior (Tronvoll et al., 1997) in the regions where reservoir rock is known to be weak, e.g. Adriatic sea and North sea. It is generally accepted that in real reservoir conditions, rock is firstly deposited and undertakes diagenesis, subsequently an oil well is drilled and then oil is produced in this formation where it is found. If the formation is shallow and weak enough, the well might start producing sand as well – this chain of events demonstrates a continuous in situ process on the same rock. Ideally, field conditions should be reconstructed in the laboratory where the whole processes of material consolidation, diagenesis, perforation, and sand production should be conducted on the same specimen when the boundary stress conditions could be controlled to simulate the real stress (re-) distribution in the field. However, many previous experiment designs of sand production usually separate the main stages of specimen preparation, perforation, and sand production. Unfortunately, the disturbance between these stages' separation causes the formation of cracks in the weak sandstone under stress release condition due to the discontinuity of confinement between these stages, as stated and investigated in the works by Holt and Kenter (1992) and Alvarado et al. (2012). Therefore, the first important feature of the newly developed apparatus presented here should have limited disturbance to the material during the transition between the main stages: specimen preparation (consolidation and cementation), saturation, in situ perforation, and sand production. For example, in the experiments by Tronvoll et al. (1997), Nicholson et al. (1998), and Papamichos et al. (2000), specimens were prepared in advance and then transferred to the testing cell, which could have caused possible cracks before sand production testing.

Another limitation of previous experiments was that the in situ perforation was usually not considered. The sand production experiments were mainly conducted using a prepared hollow cylinder specimen, and the hollow core was created by placing a metal rod in the center of the cast molds and removed after the curing process completion (Nouri et al., 2006). This method of specimen preparation limits the damaged zone during the perforation penetration, which significantly contributes to the severity of sand production (Baxter et al., 2009). Therefore, the in situ perforation should be incorporated in the apparatus design as a second development advantage.

The advantage of the presented apparatus in the current study can consider the complex fluid flow implementation since sand production behavior also depends on fluid properties and fluid flow (Nicholson et al., 1998; Papamichos et al., 2000; Wu et al., 2016). Previous experiments were usually conducted with a single fluid for one experiment, such as brine (Van Den Hoek et al., 2000; Al-Awad, 2001; Zivar et al., 2019), paraffin oil (Papamichos et al., 2000), diesel fluid (Fattahpour et al., 2012), water (Wang and Wu, 2001; Wu et al., 2016), and kerosene (Nicholson et al., 1998). In the field, both single and multiphase flows occur and this can be simplified in the experiment as a two-phase flow of water and oil to study the effect of water cut in oil (and sand) production. Implementation of two-phase fluid flow is especially crucial for oilfields where water flooding is used to maintain the reservoir pressure. Water flooding causes more sand production after water breakthrough and a distinct change in the water-to-oil-cut. The reservoir pressure is usually maintained above the wellbore pressure such that the reservoir fluid can enter the wellbore and be lifted vertically to the surface. The vertical upward flow direction affects sand production. For the case of an oil-water-sand system, depending on the fluid drag force, the produced sand particles can either be transported to the surface, suspending within the dispersed system, or be deposited to the bottom hole, which is also difficult to be predicted due to the unknown number and size of produced sand clusters. For instance, the effect of gravity on the vertical transportation of sand production is not accounted for in the experiment setup with a bottom sand trap (Fig. 1) to catch the produced sand from the specimen (Tronvoll et al., 1997; Papamichos et al., 2000; Nouri et al., 2006; Fattahpour et al., 2012). Flow direction was basically ignored in the past experiments, and therefore a vertical direction is incorporated in the current study.

Many sand production experiments in the literature were conducted on various specimens of different sizes and materials. Tronvoll et al. (1997) conducted an experiment on a synthetic sandstone specimen of 100 mm in diameter and 150 mm in height to understand the effect of stress anisotropy on sand production. Nicholson et al. (1998) experimentally studied four types of outcrop sandstone specimens with 150 mm in diameter. Papamichos et al. (2000) used a hollow cylinder apparatus accommodating sandstone specimens of 200 mm in diameter. In a recent work, Wu et al. (2016) compared sand production from three synthetic sandstones and four open-cut quarry specimens of 200 mm in diameter. In this study, a large specimen of 300 mm in diameter provides up to 2.25 times larger surface area as compared to 200 mm specimen and 9 times larger area than the commonly used 100 mm specimen. The size enlargement reduces the impact of boundary condition on the perforation and sand production results.

A new apparatus (i.e. the high pressure consolidation system, HPCS) and experimental process were developed in this context to understand the sand production behavior from the weakly consolidated reservoirs prone to sanding, particularly in Kazakhstani conditions. The tests were designed such that both the solid and fluid pressures can be controlled throughout the processes of specimen preparation (consolidation and diagenesis), perforation and sand production under multiphase fluid flow conditions. The reservoir materials are particularly weak, and no cores of sufficient quality were retrieved for testing purpose and HPCS was used to prepare a large artificial sandstone specimen, which was then used for the study of perforation and sand production with the same experimental setup to minimize disturbance to the weak material. This paper discusses the design, construction, and function of HPCS, testing procedure, and performance of the system in a sand production experiment, with the following main advantages:

(1) Limited unintentional disturbance of the specimen and a gradual transition between the main experimental stages (specimen preparation (consolidation and cementation), saturation, perforation, and sand production);
(2) Implementation of in situ perforation (with gun or drill);
(3) Single- or two-phase flow implementation;
(4) Upward outflow direction of produced fluid + sand mixture; and
(5) Large size of the specimen: 300 mm in diameter.

2. Design of high pressure consolidation system (HPCS)

The weak sandstone reservoirs in Kazakhstan are of a typical sand production problem, where no effective sand control can be used to date. The produced sands are generally disposed on the ground leading to a serious environmental problem. The reservoir rock consists of shallow marine sandstones of Lower Cretaceous age at depth of 200–500 m, which is characterized as porous, permeable, and weak. The reservoir fluid has very high viscosity (200–800 mPa s). The reservoir pressure is currently maintained at 3 MPa by water flooding, and oil is produced with high water cut values greater than 60%. The equipment was designed to replicate

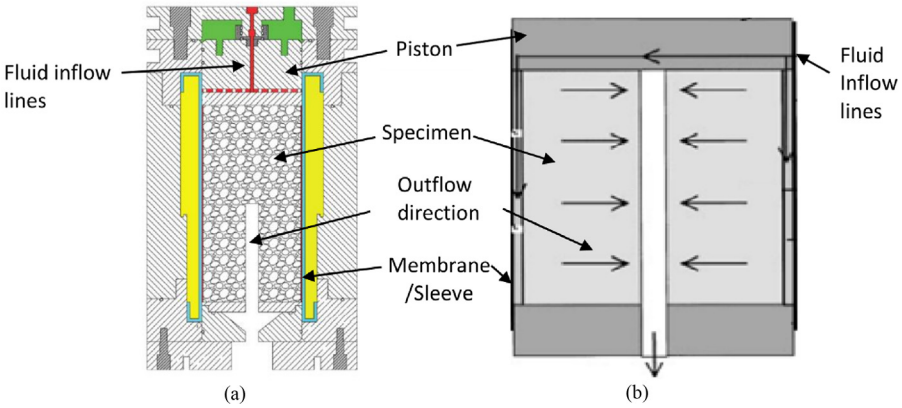

Fig. 1. A typical sand production setup with sand trap located below the cell: (a) After Fattahpour et al. (2012) and (b) After Papamichos et al. (2001).

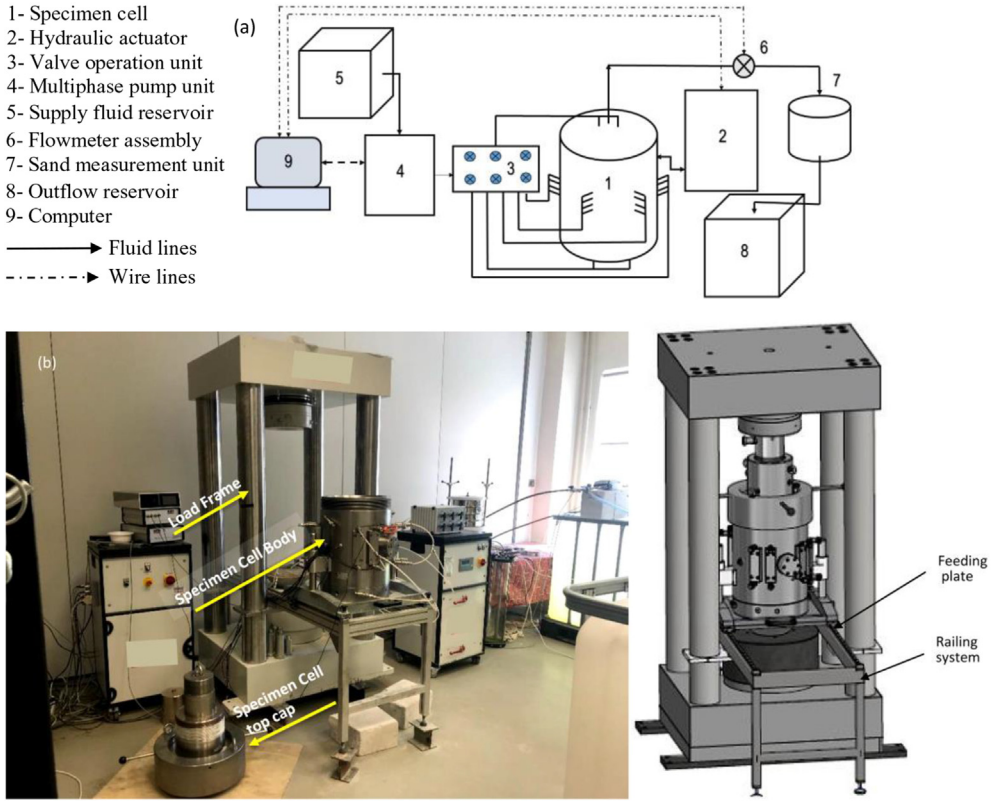

Fig. 2. High pressure consolidation system: (a) Schematic diagram, (b) General view, and (c) Specimen cell in the loading position.

the field conditions for both the solid and fluid conditions where material consolidation can be approximated by a vertical compression of similar granular material. As the vertical stress is developed to simulate the overburden stress during compression, the horizontal stress increases due to the prevented lateral expansion, which is similar to the stress condition in a Rowe Cell apparatus (Rowe and Barden, 1966) in soil mechanics. As the target overburden stress is reached, which is confirmed by the load transducer, the vertical stress is maintained by the computer-controlled loading system and the specimen is cemented inside the rigid mold under zero lateral extension for 60 min. The locked-in horizontal stress is proportional to the vertical stress, as similar to that in a diagenesis process in nature. The specimen retrieved after the test completion is homogeneous.

The HPCS is equipped with a servo-hydraulic compression load frame with loading capacity of 5000 kN (Fig. 2) to apply vertical compression force on a specimen with specified diameter placed inside a rigid cylindrical mold. The specimen under vertical compression is sandwiched between the detached top cap and the bottom cap inside the rigid cylindrical wall. The bottom cap and the wall form a hollow mold that is pushed up from the bottom by the hydraulic cylinder of the load frame such that the specimen inside is compressed by the top cap connected to the fixed top of the load frame. The specimen is prepared by placing a mixture of a chosen granular material with a cementing agent into the mold, which is

then subjected to vertical compression inside the load frame. The compression process can be applied under a stress- or strain-controlled manner following a specified rate until the target overburden stress is achieved. Cementation can be activated at any selected stress level, and curing takes place when the boundary stress condition is maintained. Natural specimens can be tested when they are trimmed to the exact dimension of the mold, although such specimens would require special extraction methods in the field.

The schematic diagram and the general view of the apparatus are shown in Fig. 2. The HPCS is fully computer-controlled for applying solid and fluid pressures. As illustrated in Fig. 2, the specimen cell is connected to the hydraulic actuator and the computer. Once the specimen is set up properly within the system, an operator only needs to specify the target vertical stress value, and an increasing rate in the controlling software and the loading will be carried out automatically. The cell is connected with the flow system, which is situated between the fluid supply reservoir and the outflow reservoir. The inflow is pressurized by the multiphase pump unit and fed into the specimen through a series of ports installed on the bottom and side of the specimen whereas outflow is directed to the top and into the outflow reservoir. Flow into the specimen can be manipulated using the valve operation unit to simulate different flow directions. Fluid flow can be injected from different ports on the cell wall and on the bottom plate such that while the radial flow can occur from the wall ports, the vertical flow can occur from the bottom ports toward the central vertical perforation. Furthermore, the wall and the bottom ports can be activated independently to allow for only one flow direction (radial or vertical) or both directions. Different fluids can be supplied from different reservoirs for the simulation of multiphase flow using the HPCS. For the multiphase flow condition, the specimen can be saturated with oil using the air/liquid pressure cylinder and the separate high-pressure pump can be used to inject water into the oil-saturated specimen during sand production. The high-pressure pump can also support multiphase flow when different fluids from different reservoirs can be mixed at the pump's inlet for more complex testing conditions. The outflow rate can be measured continuously with a flow meter (cori-flow) assembly, and the measurement can be used as the feedback information to the multiphase pump unit to adjust the inlet pressure if a constant flow is desirable in an experiment with long duration; otherwise, it provides real-time flow rate in a fluid pressure-controlled test. The produced sand particles are filtered and weighted in a sand measurement unit, and water can be sent back to the water supply system after the filtration is discarded.

The HPCS is made up of high-strength and anti-corrosive materials to maintain integrity under high-pressure testing conditions and it can resist the abrasive materials of fine sands and aggressive chemicals when brine and different crude oils are used in the experiment.

2.1. Load frame and specimen cell

The most important feature of the designed equipment is the specimen cell, with which material consolidation, diagenesis, perforation, and sand production can be conducted without removing the specimen from the cell temporarily and hence loosing the confinement and creating disturbance to the specimen. As the perforation diameter is measured as 10–20 mm, the specimen diameter should be larger than that of damaged zone due to perforation, which is assumed to be about 5 times that of the perforation (Pucknell and Behrmann, 1991). Finally, the inner diameter of the cell was created to be 300 mm. The oil-producing horizons in the local reservoirs are located at around 500 m depth; taking into account the specimen surface area, the load frame of 5000 kN capacity was used to apply the maximum vertical stress equivalent to around 3200 m depth of the reservoir.

The load frame is constructed by 4 rigid columns that provide clearance for moving the cell in and out of the loading position using a supporting frame. The dimensions of the load frame and the cell allow a maximum initial specimen height of 240 mm.

The external position in Fig. 2b is used for specimen preparation in the beginning. Perforation through the central conduit of the loading structure after the specimen is cemented, and cleaned at the end of experiment. The loading position (Fig. 2c) is used for vertical compression of specimen to simulate the consolidation and diagenesis in nature during sand production and to extrude the specimen out of the cell at the end. Note that if the consolidation stress represents the overburden stress, its removal during perforation may represent stress reduction during drilling of a horizontal well and finally it can be set to an appropriate value during sand production to reflect the real condition. Radial stress varies as a function of vertical stress change as similar to the stress situation around a vertical perforation of the horizontal well in the field.

The high pressure consolidation cell was designed for two competing requirements, i.e. (i) the necessity for access to the top surface of specimen during experiment for perforation penetration, and (ii) a liquid sealing system that can sustain a maximum fluid injection pressure of 7 MPa with the flow going toward the top central exit port above the perforation tunnel.

The cylindrical wall of the cell is shown in Fig. 3a and b. There are 8 pairs of fluid injection ports (a total of 16) installed at the locations of 22.5°, 45°, 112.5°, 135°, 202.5°, 225°, 292.5° and 315° along the circular circumference of the cell (Fig. 3c).

There are also two horizontal (radial) pressure transducers installed at 0° and 180° locations on the wall, one pair of S-wave ultrasonic sensors at 75° and another pair of P-wave ultrasonic sensors at 105° locations (inset in Fig. 3a) to measure the wave propagation properties of the material on the horizontal plane of the installation. The top of the wall is threaded to attach it to the top cap using a coupler as shown in Fig. 3a and b.

The total weight of top cap is measured 265 kg. Handling of the heavy top cap to place it on top of the cell and align both parts of the threads requires careful execution to avoid damage to such a delicate thread system. A mobile crane is used to hook the top cap up, and a spring-scale system is used in between the loading line for weight compensation, as shown in Fig. 4a and b. After the first contact between the threads of the coupler and of the cell is established, the coupler is slowly screwed to the cell threads while the spring is used to maintain a maximum of 75% the coupler weight as shown on the scale. This installation procedure assures that the applied weight cannot exceed the allowance for safe use of the threads while maintaining the vertical alignment of the top cap.

The cross-section of the top cap in Fig. 5 shows that the specimen is compressed by a guided loading column such that the loading plate is prevented from rotation and the top surface of the specimen is deformed in an equal-strain condition. There is a conduit created at the center of the loading plate and the column such that it provides an escape way for water to flow out from the specimen. There is a tiny gap between the side of the loading plate and the inner wall of the cell, where an O-ring is installed around the loading plate such that it minimizes sand particles but allows water to move through the gap. As water fills in the space between the loading plate and the coupler, there are two drainage valves to deplete air until the space is fully filled by water. It should be noted that the final design was adapted from an earlier solution when the loading plate is allowed to rotate, and this caused great frictional contact between the side of the loading plate and the sidewall. The top cap cannot be removed easily after the test as the applied force

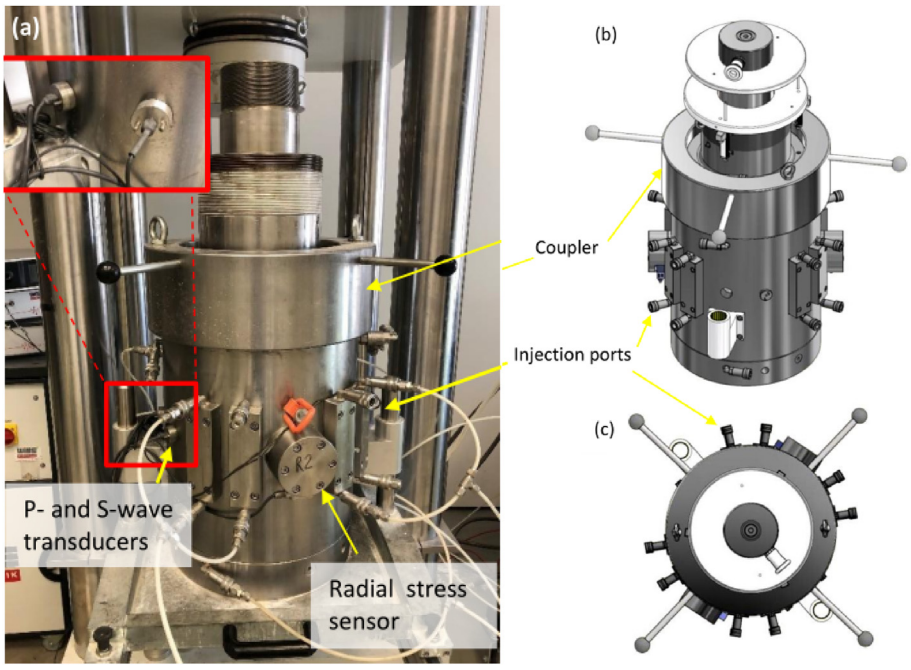

Fig. 3. High pressure consolidation cell with top cap: (a) General view, (b) Schematic orthogonal view, and (c) Schematic top view.

is as high as 5000 kN. Thus a new top cap with the coupler was invented and the new threads were added on the top part of the outside wall to satisfy the water sealing requirement.

The top cap consists of three coaxial components (Fig. 5): the coupler at the outer part, the guidance at the middle part, and the attached loading column and loading plate at the inner part. The guidance rests on top of the cell's wall and is pressed against the top surface of the wall by screwing the coupler outside. The loading column and loading plate form a reversed T-shaped structure that slides freely inside the guidance. The whole cell wall with the bottom plate, the guidance, and the coupler move up together and compress the specimen inside against the loading T-shaped structure and then against the fixed top of the load frame.

The bottom plate is detachable but fixed to the cell wall during the loading process. There is one pore pressure transducer installed and two holes are remained available for future purposes, which are occupied by dummies (Fig. 6a). Two fluid injection ports are created on the side of the bottom plate, which are connected to 30 small holes for even flow distribution during bottom fluid injection (Fig. 6b).

After the test, the top cap can be removed from the cell, and the bottom plate is unscrewed from the wall such that the specimen can be pushed up inside with the help of extrusion cylinders (Fig. 7). The extrusion cylinders are placed below the cell one by one along the specimen extrusion such that the whole specimen is lifted and can be retrieved for further analysis.

2.2. Liquid flow system

A liquid flow system is needed to saturate the specimen and to conduct the sand production test when multiphase flow is injected

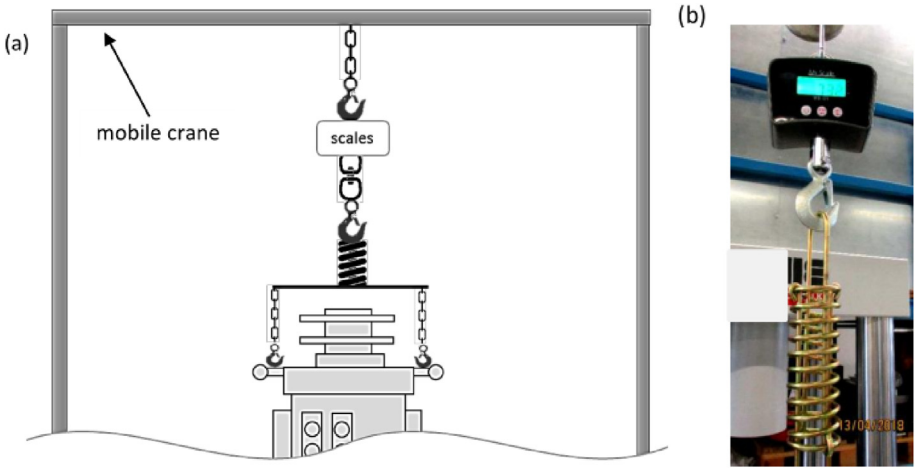

Fig. 4. Weight compensation tool of high pressure consolidation cell: (a) Schematics and (b) General view.

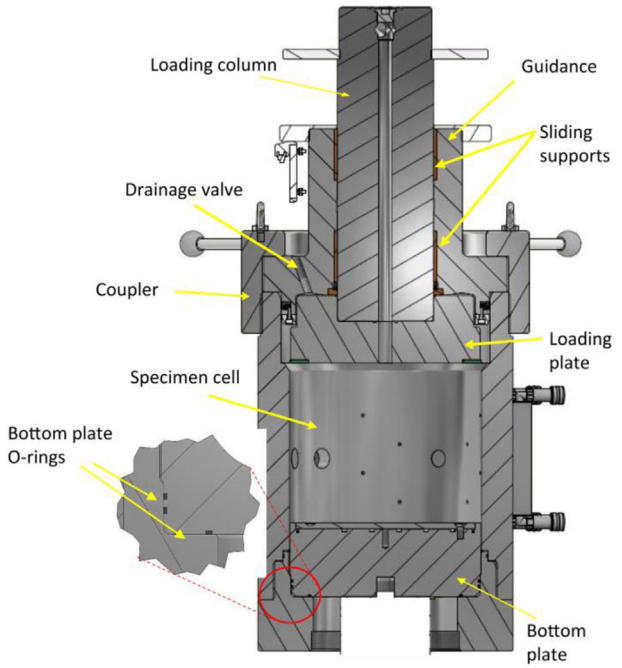

Fig. 5. High pressure consolidation cell schematics (after Wille Geotechnik, 2016).

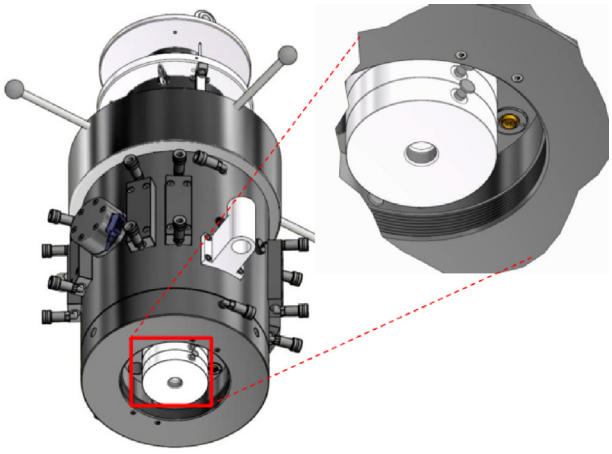

Fig. 7. Extrusion cylinders. Used for the full range flow regime, and an air/liquid pressure cylinder system (see Fig. 8b) is used for only the low flow regime.

from the boundary of the specimen in radial and/or vertical (from the bottom) directions toward the central perforation tunnel to go through the conduit embedded in the top loading structure to the outside. Sometimes a liquid cementing agent, e.g. CIPS solution (Kucharski et al., 1997), may also be used for cementation of specimen. For sand production, a high flow regime is necessary with a maximum flow rate of 5 L/min, or with a maximum injection pressure of 7 MPa. In contrast, a lower flow regime is sufficient for saturation and cement injection. The HPCS is equipped with two liquid supply systems, where a high-capacity multiphase pump (Fig. 8a) is.

For multiphase flow, there are two tanks of 1 m^3 for water and oil supply; together with the air/liquid pressure cylinder (Fig. 8b), they are all connected to the pump unit, as shown in Fig. 8a. The lower handle in Fig. 8a is used to switch between the two liquid supply systems where the left position is used for the low flow regime (no pump), and the right position is used for the high flow regime with the pump. The upper handle, on the other hand, is used with the pump, where the left position is used with supply from the water tank while the right position is for the oil tank. The larger liquid supply tanks provide longer flow conditions as the flow rate can be as high as 5 L/min. There is also an operator panel for manual control of the pump if necessary; otherwise sand production is conducted completely automatically using the control software at the computer terminal.

The pump unit is connected to a valve operation unit as shown in Fig. 8c, which directs the flow to different injection ports on the cell. “Drain” and “Fill” indicate flow direction into/out of the cell from/to the liquid tanks, whereas the vertical position indicates a closed valve. Note that the top valve was no longer used as we lost access to the top injection ports with the change of the top cap to its current form. There are four valves and hence injection lines for radial flow, which can be connected to a maximum of 50% the radial injection ports (4 out of 8 pairs in total). The bottom injection line (valve) is for the pair of injection ports in the bottom plate and the top line becomes redundant or can be used for a radial injection. The radial injection is implemented via plastic tubings with 4.7 mm

Fig. 6. Bottom plate of high pressure consolidation cell: (left) Bottom and (right) Top views.

Fig. 8. Liquid supply system: (a) Multiphase pump unit, (b) Air/liquid pressure cylinder, and (c) Valve operation unit.

inner diameter, which were designed for the high flow rate, high pressure, and aggressive liquids in the study.

The fluid flow can be regulated automatically or manually using the computer or the control panel on the pump unit, independent of applying vertical stress. The sand production experiment can simulate a pressure drawdown condition when a constant inlet pressure is set at the injection ports in the software and collect a free flow at the outlet. In another case, a constant flow rate target can be set for the output from the outflow meter such that the computer will continuously adjust the pump to attain the specified flow condition. In the latter case, we can bypass the software and computer control to set a constant injection flow rate using the control panel of the pump unit. The fluid flows through the porous media of the specimen towards the top exit, which continues to the solid filtration and collection and finally to the fluid collection tank. As the specimen is subjected to the coupled solid and hydraulic stresses during sand production, plastic deformation may take place and create free particles to be transported out with the flow. This dynamic process depends on both the initial parameters and any further variation of the solid and liquid phases during the test.

2.3. Instrumentation system

The instrumentation system was designed to allow extensive monitoring of experimental condition in terms of solid stress, specimen condition, fluid pressure, flow condition, and solid production. The monitoring results can also be used as the feedback information to adjust the operation of the load frame and the pump to implement different experimental programs.

The HPCS is equipped with a vertical load transducer (Fig. 9a) and a vertical displacement transducer (Fig. 9b) associated with the hydraulic servo actuator of the load frame. The vertical stress is calculated from the vertical load and the specimen area automatically and displayed in the software with a measurement sensitivity of 0.1 kPa. The vertical displacement transducer is a potentiometer

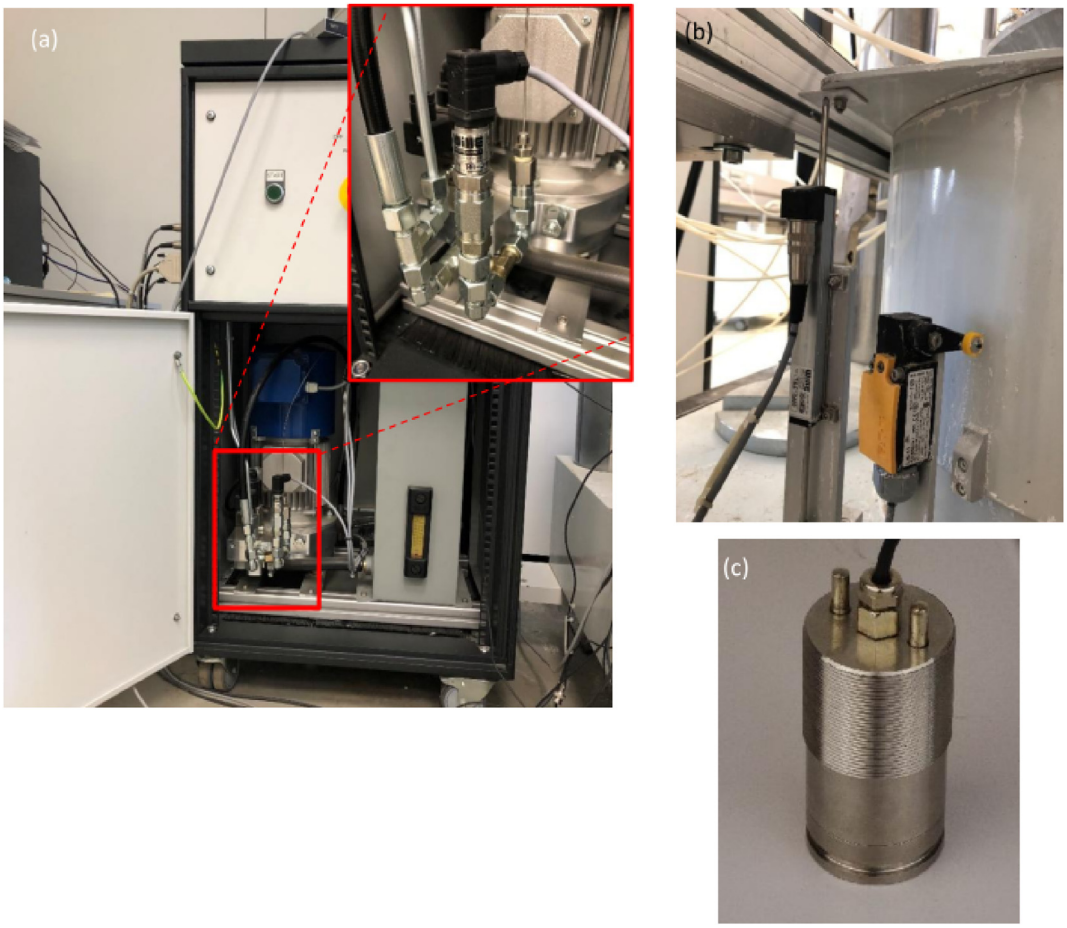

Fig. 9. Instrumentation system: (a) Vertical load transducer, (b) Vertical displacement transducer, and (c) Ultrasonic transducer.

that has a measurement range of 0–100 mm with linearity of 0.15%. The measurement from these sensors is used to drive the actuator in either stress- or strain-controlled fashion. If the applied vertical stress on the specimen is measured indirectly from the actuator, the radial stress is measured directly by two radial stress sensors installed opposite to each other on the cell wall such that there is direct contact between the side of the specimen and the diaphragm of the pressure sensor.

The condition of the specimen can be measured in terms of ultrasonic pulse velocity by a pair of P- and S-wave transducers (Fig. 9c) installed on the cell wall (Fig. 3a) as similar to the radial stress transducer. The non-destructive measurement technique allows calculation of compression and shear wave velocities from the travel time and the distance between the transmitter and the receiver of the sensor. The velocity values can be used to estimate the elastic properties of the material, along with the porosity, density and compressive strength of rocks (Rafavich et al., 1984; Vernik and Nur, 1992; Yasar and Erdogan, 2004; Garia et al., 2019), which is a common practice used in the oil and gas industry. The P- and S-wave transducers have the frequency range of 0.5–1.5 MHz, a nominal operating voltage of 60 V and a maximum operating voltage of 300 V. Special mechanical design of the sensor allows for an operating temperature in the range of −10 °C–60 °C and a pressure resistance up to 10 MPa.

The behaviors of the porous soil and rock are dependent on the pore pressure, which can be described in terms of effective stress as the difference between the total solid stress and pore pressure for the case of full saturation. Measurement of pore pressure is important for the calculation of effective stress and for checking the saturation of the specimen in no-flow condition as compared to the inlet and outlet pressures. A piezoresistive pore pressure transducer was installed in the bottom plate of the cell to measure the

Fig. 10. Fluid outflow direction.

pore pressure inside the specimen with a precision of 0.001% under room temperature condition.

The outflow goes through the conduits inside the loading column of the top cap and continues to the outside via an elbow fitting, as shown in Fig. 10, provided that sufficient hydrostatic head is applied. Once the sand particles are produced with the flow, the velocity needs to be higher than a critical velocity to uplift the smallest particles in the slurry, which is similar to the well situation in the field. The outflow line is extended, as shown in Fig. 11, which includes, along the line, a bypass valve, a sand filter, an outlet pressure transducer, a flow regulator, and a flow meter. Note that flow rate data are also provided directly from the pump unit to the software and two measured flow rates should be the same for a steady-state flow. The sand filter is used to trap coarse solids larger than 400 μm to protect the outlet pressure transducer in case they are produced as bonded sand clusters that are out of the range of the particle size distribution. The flow regulator can be used to precisely adjust the outlet pressure to attain an exact pressure drawdown between the inlet and outlet pressures. The bypass valve is used when there is massive sand production that blocks the filter and stops the flow in some cases. A summary of the technical specification of the sensors is given in Table 1.

The mass of the produced sands is measured using a sand measurement unit, as shown in Fig. 12. After passing through the flow meter, the liquid together with the dispersed sand particles flows inside a flexible plastic tube directly onto a fine mesh suspended sieve (which captures the particles but not the liquid) located near the bottom of the water tank (Fig. 12b and c). The sieve is supported by an independent frame that can be placed on a scale such that the sand mass can be measured as the difference in the scale measurements between a no-sand and a sanding condition. The liquid, on the other hand, is contained within the tank, which is supported on an entirely different structure, and discharged when the liquid reaches an upper level, as shown in Fig. 12a. This device allows for the measurement of the produced sand in real-time (with manual recording), which is similar to the design approach by Fattahpour et al. (2012). The fluid flow going out of the unit can be either discarded or sent back to the liquid supply reservoir. The produced sands can be collected from the sieve at the end of the experiment for further analysis.

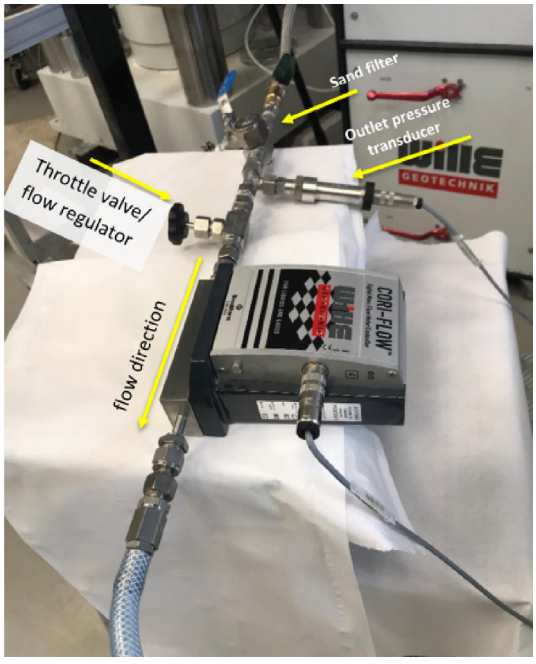

Fig. 11. Devices installed at the outlet.

3. HPCS performance from the results of an integrated experiment

3.1. Specimen preparation

The artificial sandstone can be prepared directly inside the cell. To simulate the in situ cementation in the natural reservoir, two cementing agents were implemented with the HPCS: the proprietary calcite in situ precipitation system (CIPS) (Kucharski et al., 1997; Ismail et al., 2000) and the silicate solution (Holt and Kenter, 1992; Holt et al., 1993; Tronvoll et al., 1993). In the presented case, the specimen was prepared with the silicate solution method. First, sand and sodium silicate solution were mixed thoroughly following a 10:1 sand to silicate solution ratio. According to the size of the cell, the initial mixture was prepared with 23 kg sand and 2.3 kg sodium silicate solution. We used a silica open quarry sand, which was clean and poorly graded, with the mean grain size of 0.3 mm, coefficient of uniformity of 2 and coefficient of curvature equal to 0.89. The mixture was then placed into the cell in a sequence of 5 layers, and each layer was compressed lightly to ensure the even distribution of the mixture. The fluid injection ports on the wall were covered by filter paper to prevent the escape of fine sand particles into the components that may cause leakage under high fluid pressure application during the later experimental stages. The discontinuity between different layers was minimized by scratching the surface of each layer before placing the next layer. After the total mixture was placed (Fig. 13a), the top cap was attached to the cell's body, and the cell completely slid into the loading position within the load frame using a special feeding plate that rides on a railing system as shown in Fig. 1c.

The specimen was initially compressed vertically with zero lateral expansion due to the rigid cell. The drainage valve in the top cap was left open to deplete air out of the specimen. The specimen was compressed until a target vertical stress of 1000 kPa and was maintained in this condition until the recorded vertical settlement ceased to change (Fig. 14).

The in situ cementation (Fig. 15) was then activated by injecting carbon dioxide (CO_2) from an industrial gas cylinder to the cell through the injection ports and bypassed the pump using the lower handle in Fig. 8a. Note that the CO_2 gas cylinder was used here instead of the air/liquid pressure cylinder, which was reserved for the case of a liquid cementing agent (i.e. CIPS). The CO_2 gas was injected into the specimen at point 1 in Fig. 15 and percolated through the specimen for 40–60 min, when the outlet valve was left open, at a rate of 5 L/min and under a 500 kPa pressure. The radial stresses increase from the values at the end of the consolidation in Fig. 14, while the vertical stress does not change as it is maintained by the computer-controlled loading system. The cement bonds were created in the form of silicic acid that results from the chemical reaction between the sodium silicate and the CO_2 gas (Holt et al., 1993), which can be given as

$$Na_2Si_3O_7 + 2H_2O + 2CO_2 \rightarrow 3SiO_2 \cdot H_2O + 2NaHCO_3$$

The mole ratio of the sodium silicate solution and CO_2 is equal to their mass ratio. Approximately 293 g or 148 L CO_2 is needed to react with 2.3 kg sodium silicate solution mixed inside the specimen, and that can be provided by maintaining the CO_2 gas pressure injected into the specimen while the outlet valve was closed for 25–30 min between points 2 and 3 in Fig. 15. The radial stress measurements fluctuated when the gas flow started and then was switched off during the cementation process. A greater residual

Table 1
Technical specification of the sensors used in the HPCS.

No.	Sensor	Transducer type	Specification
1	Pore water pressure, pump inflow pressure and outlet pressure	Piezoresistive	Output signal: 0–10 V, RS482 Pressure connection: G1/4″ Electrical connection: Binder 723/5-p Supply: 13–32 V Error: 0.01% FS@25 °C; 0.003%FS@10 °C-40 °C
2	Radial stress	Strain gage piezoresistive	Force: 25 kN Size of the sensor: ϕ100 mm × 35 mm Linearity hysteresis: ±0.05%FS Supply: 0–28 V, 30 mA
3	Vertical displacement	Potentiometer	Measurement range: 0–100 mm Repeat accuracy: 2 μm Linearity: 0.15% Maximum supply: 42 V
4	Vertical load	Piezoresistive	Output signal: 0–10 V, RS482 Pressure connection: G1/4″ Electrical connection: Binder 723/5-p Supply: 13–32 V
5	Ultrasonic waves propagation	Piezoelectric	Frequency range: 1 MHz (0.5–1.5 MHz) Interface: BNC Minimum sizes: 31.5 mm × 63.5 mm
6	Flow meter	Coriolis measurement principle for oil, water and oil-water emulsions	Stainless steel pipes Flow rate: 0.5–5 L/min Precision: < 1% Supply: +15–24 V Output: 0–100% (digital RS-232), 0–10 V (analog)

Note: FS means the full-scale.

stress value was reached at the end of the cementation, which could reflect a volume expansion tendency due to cementation. Vertical stress, on the other hand, was constant throughout the whole process as it was maintained by the control system of the load frame. The cementation process was considered complete when all readings became flat.

3.2. Specimen saturation and perforation

Once the cemented specimen was formed, the cell was removed from the load frame such that the top cap could be lifted up to gain access to the top surface of the specimen (Fig. 13b). The height of the specimen was measured for successive void ratio calculation based on the specimen dimension and its mass (Rocchi and Coop, 2014). A piece of donut-shaped filter paper was placed on the top surface of the specimen, the top cap was closed again, and the specimen returned to the loading position. Water was circulated through the specimen by injecting it at a low flow rate from the bottom to avoid disturbance to the weak porous material. The top drainage valve was left open until the upper chamber in the top cap was fully filled by water. The fluid circulation was kept until the circulated volume exceeded two times the cell volume. The saturation process started by closing the outlet valve and increased the injection pressure as similar to the application of backpressure in the triaxial test. Inlet pressure was increased in steps while monitoring the pore pressure and the outlet pressure readings. The equilibration of injection, pore and outlet pressures would indicate a full saturation; otherwise, the inlet pressure was maintained as high as 700 kPa overnight.

The specimen was removed from the loading position so that it could be perforated using a penetrometer that slid inside the conduit of the top cap in Fig. 5. For simplicity, in this case, a long drill bit of 14 mm in diameter was used instead of a penetrometer to drill a central vertical hole along the full height of the specimen to act as the perforation tunnel. The perforation damage hence was minimized in the drilling as compared to a mechanical penetration or a perforation gun in the field. The perforated specimen returned again to the loading position and was ready for the stage of sand production experiment. Note that during the saturation and perforation stages, the specimen was removed multiple times from the loading position, which could affect the initially applied overburden stress. The removal of overburden stress, however, also occurs in the field during the drilling and cementing operations of a horizontal well. The radial stress, on the other hand, was locked-in due to the specimen cell as similar to the horizontal stress condition in the wall along the well's axis. Once inside the load frame, application of the vertical stress can be resumed according to the experimental program.

3.3. Sand production under different flow rates

The perforated specimen was utilized to conduct the sand production experiment where water was injected from the injection ports on the cell such that water (together with sand) was produced at the outlet under a specified pressure drawdown. The experiment was divided into several stages of different vertical stresses applied to simulate different producing horizons (depth) in the field. In each stage, the pressure drawdown was applied and kept constant when we measured the fluid flow rate and the amount of produced sand (if any). The pressure drawdown was then increased to study the effects of drawdown and flow rate on the sand production behavior. A summary of the experimental stages is given in Table 2, which includes the information of the applied vertical stress, drawdown pressure, fluid flow rate, and sand production.

The fluid flow started with a small flow rate of 0.9 L/min to lift up and remove the sand debris created during perforation before the first sand production stage. In stage A, vertical stress of 1000 kPa was applied, and then a pressure drawdown of 100 kPa was applied, which produced a steady-state fluid flow rate of 1.2 L/min for around 20 min, but no sand was observed. The drawdown pressure was increased to 400 kPa and subsequently to 800 kPa, and the test continued in a similar fashion, but still no sand was observed at 2.7 L/min flow rate. It is concluded that sand is not produced at this overburden stress level and in this drawdown pressure range, which is comparable to the field result. The flow was ceased slowly and the vertical stress was increased to 2000 kPa in the stage B. Different drawdown pressures were applied as shown in Table 2, yet similarly no sand was collected for fluid rate of 2.6 L/min. The flow was again ceased and the vertical stress was increased to 3000 kPa in stage C, during which 1.1 g sand burst was first collected at 2.4 L/min flow rate and another sand burst of 0.8 g was obtained when the flow rate was increased to 2.8 L/min. The experimental results of stage C are shown in Fig. 16, and the

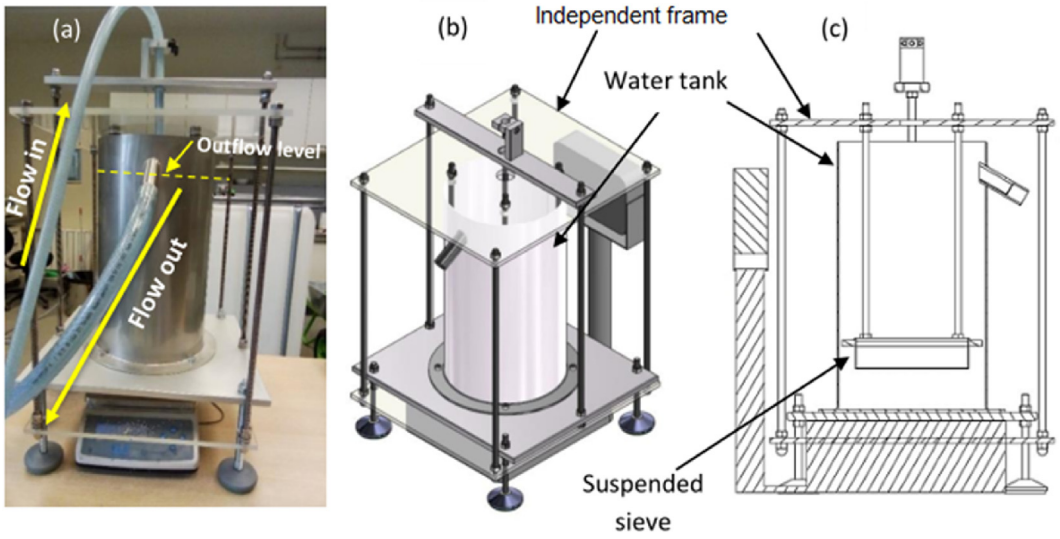

Fig. 12. Sand measurement unit: (a) General view, (b) Schematic orthogonal view, and (c) Side view (after Wille Geotechnik, 2016).

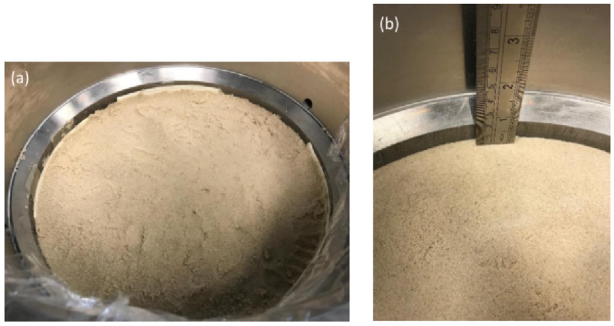

Fig. 13. Specimen preparation: (a) Initial state, and (b) Cemented sandstone specimen.

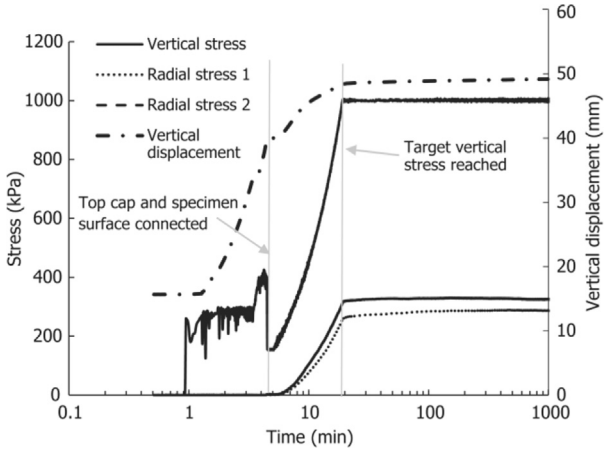

Fig. 14. Distribution of vertical and radial stresses during consolidation.

produced sand pattern is similar to that usually observed in oil fields, i.e. increase in flow rate leads to increase in the cumulative sand production with the increment being smaller with each successive increase.

The experimental results from the HPCS equipment can be used for development of analytical models for prediction of sand production (e.g. Kozhagulova et al., 2020a; Shabdirova et al., 2020). Material properties of the same cemented sandstone obtained from a set of triaxial tests (Kozhagulova et al., 2020b) were utilized to predict the material failure. The results were combined with the measurements of sand mass and sanding rate in the sand production experiments to develop and calibrate analytical models for prediction of sanding onset and sand volume for the ranges of fluid flow rate, solid stresses, and pressure drawdown in this study.

Fig. 17 shows the extruded specimen after the test with some of the filter papers still being remained in-place. The filter papers were used to prevent the fine sand particles going into the ports and causing leakage, and the top paper was used to prevent surface erosion as observed in some tests. The produced sand hence came from the perforation and the plastic zone around the cavity (Risnes et al., 1982), due to the applied stress distribution and the interaction with the hydrodynamic forces of the fluid flow in this zone. The retrieved specimen can be used for further analysis of microstructural change inside the specimen as the result of sand production.

4. Conclusions

A new apparatus and a novel experimental method were developed to understand the sanding behavior in weak sandstone reservoirs in Kazakhstan. Through replicating the realistic rock diagenesis, perforation, and sand production processes in the field using a single large artificial specimen, a comprehensive study of the sand production phenomenon was conducted, where the solid and fluid pressures and flows were entirely computer-controlled and monitored during the whole experiment. The HPCS also allows the study of both single and multiphase flows in porous media at realistic reservoir pressures to simulate different scenarios in a well's life, for example, by implementing different depletion and/or water-to-oil cuts. The results of the integrated experiment on an artificial sandstone prepared with sodium silicate cementing agent were presented in three successive steps of specimen preparation with in situ cementation, perforation under a realistic boundary stress condition, and sand production with ramp-up pressure drawdown and flow rate. The observed sand production patterns in the laboratory were similar to the actual sand production behavior in the local fields where a critical flow rate is required to trigger

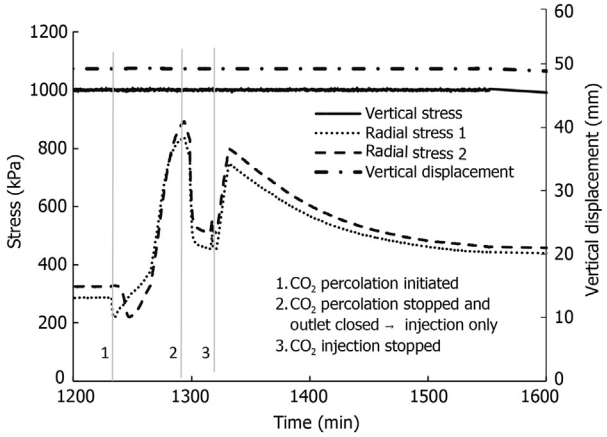

Fig. 15. Distributions of vertical and radial stresses during cementation.

Fig. 17. The specimen retrieved after the test.

Table 2
Summary of sand production test stages.

Stage	Vertical stress (kPa)	Drawdown pressure (kPa)	Fluid flow rate (L/min)	Produced sand (g)
A	1000	100	1.2	–
		400	1.9	–
		800	2.7	–
B	2000	75	0.9	–
		380	1.7	–
		750	2.6	–
C	3000	55	0.6	–
		360	1.5	–
		560	2	–
		730	2.4	1.1
		950	2.8	0.8

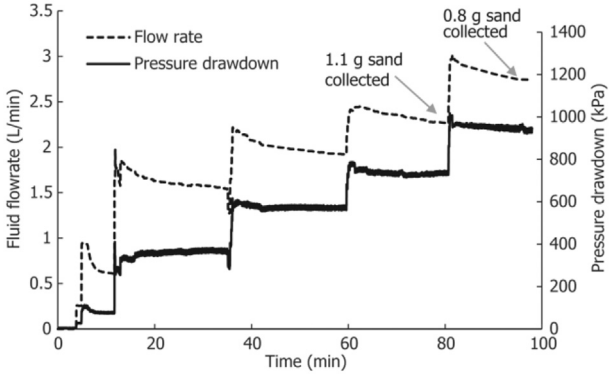

Fig. 16. Sand production behavior under successive increases of pressure drawdown in stage C.

sand production and a subsequent increase above the critical flow rate will create another, albeit smaller, sand burst. The material and sand production studies provided valuable insight into the sand production in the local weak sandstone reservoirs for development of analytical models that can successfully predict the actual sand production (Kozhagulova et al., 2020a; Shabdirova et al., 2020). The study of multiphase flow effect on sand production is being carried out, which will provide another critical development on the prediction of sand production in the depleting reservoirs.

Declaration of competing interest

The authors declare that they have no known competing financial interests or personal relationships that could have appeared to influence the work reported in this paper.

Acknowledgments

The authors acknowledge the financial support from Nazarbayev University (Grant No. SOE2015004) and Ministry of Education and Science of the Republic of Kazakhstan (Grant No. AP08052762).

References

Al-Awad, M.N.J., 2001. The mechanism of sand production caused by pore pressure fluctuations. Oil Gas Sci Technol. 56 (4), 339–345.
Alvarado, G., Coop, M.R., Willson, S., 2012. On the role of bond breakage due to unloading in the behaviour of weak sandstones. Géotechnique 62 (4), 303–316.
Baxter, D., Behrmann, L.A., Grove, B., Williams, H., Heiland, J., Hong, L.J., Khong, C.K., Martin, A., Mishra, V.K., Munro, J., Pizzolante, I., Safiin, N., Suppiah, R.R., 2009. Perforating – when failure is the objective. Oilfield Rev. 21 (3), 4–17.
Fattahpour, V., Moosavi, M., Mehranpour, M., 2012. An experimental investigation on the effect of rock strength and perforation size on sand production. J. Petrol. Sci. Eng. 86–87, 172–189.
Garia, S., Pal, A.K., Ravi, K., Nair, A.M., 2019. A comprehensive analysis on the relationships between elastic wave velocities and petrophysical properties of sedimentary rocks based on laboratory measurements. J. Petrol. Explor. Prod. Technol. 9 (3), 1869–1881.
Geotechnik, Wille, 2016. Instructions for Use High Pressure Consolidation System. APS Antriebs- Prüf- und Steuertechnik GmbH.
Hall, C.D., Harrisberger, W.H., 1970. Stability of sand arches: a key to sand control. J. Petrol. Technol. 22 (7), 821–829.
Holt, R.M., Kenter, C.J., 1992. Laboratory simulation of core damage induced by stress release. In: Tillerson, J.R., Waversik, W.R. (Eds.), Rock Mechanics - Proceedings of the 33rd U.S. Symposium on Rock Mechanics (USRMS). A.A. Balkema, Rotterdam, Netherlands, pp. 959–968.
Holt, R.M., Unander, T.E., Kenter, C.J., 1993. Constitutive mechanical behaviour of synthetic sandstone formed under stress. Int. J. Rock Mech. Min. Sci. Geomech. Abstr. 30 (7), 719–722.
Ismail, M.A., Joer, H.A., Randolph, M.F., 2000. Sample preparation technique for artificially cemented soils. Geotech. Test J. 23 (2), 171–177.
Kozhagulova, A., Minh, N.H., Zhao, Y., Fok, S.C., 2020a. Experimental and analytical investigation of sand production in weak formations for multiple well shut-ins. J. Petrol. Sci. Eng. 195, 107628. https://doi.org/10.1016/j.petrol.2020.107628.
Kozhagulova, A., Minh, N.H., Zhao, Y., Fok, S.C., 2020b. A study on bond breakage behavior of weak Cretaceous Kazakhstani reservoir sandstone analogue. Geo-

mech. Energy Environ. 21, 100159. https://doi.org/10.1016/j.gete.2019.100159.
Kucharski, E., Price, G., Li, H., Joer, H., 1997. Engineering properties of CIPS cemented calcareous sand. In: Contemporary Lithic Motion, Seismic Geology: Proceedings of the 30th International Geological Congress. CRC Press, pp. 449–460.
Nicholson, E.D., Goldsmith, G., Cook, J.M., 1998. Direct observation and modeling of sand production processes in weak sandstone. In: SPE/ISRM Rock Mechanics in Petroleum Engineering. Society of Petroleum Engineers (SPE). https://doi.org/10.2118/47328-MS.
Nouri, A., Vaziri, H., Belhaj, H., Islam, M.R., 2006. Sand-production prediction: a new set of criteria for modeling based on large-scale transient experiments and numerical investigation. SPE J. 11 (2), 227–237.
Papamichos, E., Skjærstein, A., Tronvoll, J., 2000. A volumetric sand production experiment. In: Girard, J.M., Leibman, M., Breeds, C., Doe, T. (Eds.), Pacific Rocks 2000: Rock Around the Rim - Proceedings of the 4th North American Rock Mechanics symposium (NARMS 2000). A.A. Balkema, Brookfield, USA, pp. 303–310.
Papamichos, E., Vardoulakis, I., Tronvoll, J., Skjærstein, A., 2001. Volumetric sand production model and experiment. Int. J. Numer. Anal. Methods Geomech. 25 (8), 789–808.
Pucknell, J.K., Behrmann, L.A., 1991. An investigation of the damaged zone created by perforating. In: SPE Annual Technical Conference and Exhibition. SPE, pp. 511–522. https://doi.org/10.2118/22811-MS.
Rafavich, F., Kendall, C.H.S.C., Todd, T.P., 1984. The relationship between acoustic properties and the petrographic character of carbonate rocks. Geophysics 49 (10), 1622–1636.
Risnes, R., Bratli, R.K., Horsrud, P., 1982. Sand stresses around a wellbore. SPE J. 22 (6), 883–898.
Rocchi, I., Coop, M.R., 2014. Experimental accuracy of the initial specific volume. Geotech. Test J. 37 (1), 169–175.
Rowe, P.W., Barden, L., 1966. A new consolidation cell. Géotechnique 16 (2), 162–170.
Shabdirova, A.D., Khamitov, F.A., Kozhagulova, A.A., Amanbek, Y., Minh, N.H., Zhao, Y., 2020. Experimental and numerical investigation of the plastic zone permeability. In: 54th US Rock Mechanics/Geomechanics Symposium. Golden, USA.
Terzaghi, K., 1936. Stress distribution in dry and in saturated sand above a yielding trap-door. In: Proceedings of the 1st International Conference on Soil Mechanics and Foundation Engineering. Harvard University, Cambridge, USA, pp. 307–311.
Tronvoll, J., Kessler, N., Morita, N., Fjær, A., Santarelli, F.J., 1993. The effect of anisotropic stress state on the stability of perforation cavities. Int. J. Rock Mech. Min. Sci. Geomech. Abstr. 30 (7), 1085–1089.
Tronvoll, J., Skjaerstein, A., Papamichos, E., 1997. Sand production: mechanical failure or hydrodynamic erosion. Int. J. Rock Mech. Min. Sci. 34 (3–4), 291 e1–291.e17.
Van Den Hoek, P.J., Kooijman, A.P., De Bree, P., Kenter, C.J., Zheng, Z., Khodaverdian, M., 2000. Horizontal-wellbore stability and sand production in weakly consolidated sandstones. SPE Drilling and Completion 15 (4), 274–283.
Vernik, L., Nur, A., 1992. Petrophysical classification of siliciclastics for lithology and porosity prediction from seismic velocities. AAP Bull. 76 (9), 1295–1309.
Wang, Y., Wu, B., 2001. Boroheole collaplse and sand production evaluation: experimental testing, analytical solutions and field implications. In: DC Rocks 2001, the 38th U.S. Symposium on Rock Mechanics (USRMS). American Rock Mechanics Association (ARMA).
Wu, B., Choi, S.K., Denke, R., Barton, T., Viswanathan, C., Lim, S., Zamberi, M., Shaffee, S., Fadhlan, N., Johar, Z., Jadid, M.B., Madon, B.B., 2016. A new and practical model for amount and rate of sand production. In: Offshore Technology Conference Asia. Kuala Lumpur, Malaysia. https://doi.org/10.4043/26508-MS.
Yasar, E., Erdogan, Y., 2004. Correlating sound velocity with the density, compressive strength and Young's modulus of carbonate rocks. Int. J. Rock Mech. Min. Sci. 41 (5), 871–875.
Zivar, D., Shad, S., Foroozesh, J., Salmanpour, S., 2019. Experimental study of sand production and permeability enhancement of unconsolidated rocks under different stress conditions. J. Petrol. Sci. Eng. 181, 106238. https://doi.org/10.1016/j.petrol.2019.106238.

Ashirgul Kozhagulova is a PhD candidate at the School of Engineering and Digital Sciences at Nazarbayev University, Kazakhstan. She holds an MSc degree in Petroleum Engineering from Heriot-Watt University, UK. Currently, she investigates the sand production problems in weakly consolidated formations using experimental and analytical approaches. Previously she was a part of the regional geology team in a subsidiary of a national petroleum company.Ashirgul Kozhagulova is a PhD candidate at the School of Engineering and Digital Sciences at Nazarbayev University, Kazakhstan. She holds an MSc degree in Petroleum Engineering from Heriot-Watt University, UK. Currently, she investigates the sand production problems in weakly consolidated formations using experimental and analytical approaches. Previously she was a part of the regional geology team in a subsidiary of a national petroleum company.